

Formal Verification of CNN-based Perception Systems

Panagiotis Kouvaros and Alessio Lomuscio

Department of Computing, Imperial College London, UK

{p.kouvaros, a.lomuscio}@imperial.ac.uk

Abstract

We address the problem of verifying neural-based perception systems implemented by convolutional neural networks. We define a notion of local robustness based on affine and photometric transformations. We show the notion cannot be captured by previously employed notions of robustness. The method proposed is based on reachability analysis for feed-forward neural networks and relies on MILP encodings of both the CNNs and transformations under question. We present an implementation and discuss the experimental results obtained for a CNN trained from the MNIST data set.

1 Introduction

Autonomous systems are forecasted to revolutionise key aspects of modern life including mobility, logistics, and beyond. While considerable progress has been made on the underlying technology, severe concerns remain about the safety of the autonomous systems under development.

One of the difficulties with forthcoming autonomous systems is that they incorporate complex components that are not programmed by engineers, but are synthesised from data via machine learning methods (often called *learning-enabled components*). Additionally, there is an increasing trend to deploy autonomous systems in safety-critical areas including autonomous vehicles. These two aspects taken together call for the development of rigorous methods for the formal verification of autonomous systems based on learning-enabled components, see, e.g., DARPA's Assured Autonomy program¹.

¹<https://www.darpa.mil/program/assured-autonomy>.

One of the most widely considered architectures combining traditionally programmed and learning-enabled components is control systems (or decision making and planning modules) paired with perception systems based on data-trained classifiers. Forthcoming autonomous vehicles, among other systems, use this architecture. While there are methods to formally assess the adequacy of decision making and control components, no existing technique can provide formal guarantees about the correctness of perception systems based on machine learning methods. Not only this makes it hard to formally establish the correctness of perception systems before deployment, it also impedes the provision of formal assurances on the overall autonomous system, since the control components normally receive input from the classifiers of the perception component.

In this paper we aim to make a contribution towards solving this problem. Specifically, we introduce a method to give formal guarantees to perception systems based on convolutional neural networks (CNNs) [8]. Towards this end, we develop a concept of robustness for CNN-based perception systems with respect to affine and photometric transformations, i.e., changes in the position and colour patterns of the image. These can be used to anticipate the natural variability of the input to the perception mechanism when the system is deployed. Intuitively, establishing that for all the possible transformations of the input (up to a certain measure) the CNN classifies the image in the same way helps us understand the robustness of the perception system with respect to said transformations. Moreover, whenever misclassifications are found, these can usefully be used to retrain the network and improve its accuracy. The method we introduce relies on recasting the problem in mixed-integer linear programming (MILP) and leverages on recent work on reachability analysis for

feed-forward neural networks, which we extend here to CNNs. Two key features of our approach which make it different from recent approaches discussed below are that: (i) we study robustness with respect to image transformations as opposed to pixel alterations, (2) the method is complete, i.e., if a misclassification exists with respect to a transformation the method is theoretically guaranteed to find it. Completeness is particularly important for the purposes of guaranteeing correctness.

The rest of the paper is organised as follows. After discussing related work below, in Section 2 we introduce CNNs and image transformations. In Section 3 we develop the concept of local transformational robustness and give examples of applications. We turn to the verification problem for CNN-based classifiers in Section 4 where we construct the MILP encoding of the problem and show the soundness and completeness of the approach. We present an implementation in Section 5 and report experimental results obtained for a CNN trained from the MNIST dataset. We conclude in Section 6.

Related Work. The notions of affine and photometric transformations are well understood in the literature [11, 21]. Classifiers are normally evaluated in static terms against false positives and false negatives [3]. While these studies are relevant, they do not have the same aim as ours, which is to formally assess the correctness of a classifier with respect to image transformations.

More relevant to our aims is the recent work [7] on the verification of feed-forward networks, which includes a section on the local robustness of CNN-based classifiers. This work differs from ours in several respects. Firstly, local robustness, as defined there, captures regions (or abstract domains) of image perturbations. Differently, we here deal with a wide range of geometric and photometric transformations. If we were to express these by means of abstract domains, we would have to over-approximate the input domain, thereby obtaining robustness violations not relevant to the transformations under analysis. Instead, by developing the concept of local transformational robustness we can provide tighter notions of correctness than by purely working on local robustness. The technical details of the two approaches are also different. While [7] uses abstract interpretation as underlying method we here compile into MILP problems. While abstract interpretation provides better performance than MILP, it comes at the cost of completeness, which is a key requirement for

the purposes of verification.

Related to this, there is a fast increasing body of research addressing reachability and robustness analysis for neural networks [13, 6, 16, 15, 12]. While our approach is similar in terms of the underlying method, the aims are different since, rather than analysing reachability and robustness in abstract terms, we here intend to contribute to the concrete problem of verifying learning-enabled perception modules. When perception systems are considered in these works, they are assessed with respect to pixel variations of the images and not transformations as we do here. We are not the first to suggest that image transformations should be considered when assessing the robustness of image classifiers. This point was raised very recently also by [20] (referred to there as “semantic invariance”). However, that work is intended as initial foundational work and proposes no method to solve the problem.

Related to this submission is also the unpublished [18] which proposes a generic framework for evaluating the safety of computer vision systems. In common with this paper it aims to establish correctness of a classification with respect to image transformations. Differently from ours, their approach however is based on heuristic search for counterexamples. While it is shown to provide advantages over previous state-of-the-art based on gradient-based methods, it is necessarily incomplete, i.e., the method cannot give guarantees that if a misclassification exists this will be found. In contrast we here focus on completeness as a requirement, i.e., we guarantee that (up to computational power) *any and all* misclassifications will be found by the method. We cannot compare experimental results to [18] as the paper is unpublished and we do not have access to the tool described therein.

Lastly, as it will be clear from the rest of the paper, by using the results here presented, whenever we identify that a perception module is not robust, i.e., it classifies images differently following small transformations, our procedures return the witness of this misclassification. This can be seen as an adversarial example, see, e.g. [17], for the relevant classifier. Research in adversarial examples directly aims at finding these counterexamples. However, none of these methods is complete, hence they cannot be used to show formal correctness which is the primary aim of this work.

2 Preliminaries

Learning-enabled components for perception are typically image classifiers implemented via CNNs. We here summarise CNNs, CNN-defined image classifiers, and define image transformations as distortions. We refer to [8, 19] for more details.

CNNs are directed acyclic graphs whose nodes are structured in layers. The first layer is said to be the *input layer*, the last layer is referred to as the *output layer*, and every layer in-between is called a *hidden layer*. Every layer is either a *fully connected layer* or a *convolutional layer*.

Each node of a fully connected layer is connected to every node in the preceding layer, whereas every node of a convolutional layer is only connected to a *rectangular neighbourhood* of nodes in the preceding layer. In either case every connection is associated with a weight.

A fully connected layer is composed of two phases, whereas a convolutional layer comprises three phases. In both cases the first phase linearly activates the nodes by outputting the weighted sum of their inputs, and the second phase applies a non-linear *activation function* to the linear activation. Here we consider the Rectified Linear Unit (ReLU) whose output is the maximum between 0 and the linear activation. The third phase of a convolutional layer further applies a *pooling function* to collapse rectangular neighborhoods of activations into *representative activations*. Here we focus on the max-pooling function where the maximum activation is chosen as the representative one.

CNNs are routinely used to solve image classification problems. The problem concerns the approximation of an unspecified function $f^*: \mathbb{R}^{\alpha \times \beta \times \gamma} \rightarrow \{1, \dots, c\}$ that takes as input an image \overline{im} from an unknown distribution $\mathbb{R}^{\alpha \times \beta \times \gamma}$ (where $\alpha \times \beta$ are the pixels of the image and γ is the number of the color bands, e.g. RGB) and determines among a set of classes $\{1, \dots, c\}$ the class to which \overline{im} is a member. The problem is tackled by training a CNN by means of a labelled training set thereby setting the weights of the network so that its output approximates f^* [8]. Following this, the CNN can be used to infer the class of novel images by feeding an image to the input layer and then propagating it through the network. At each step the outputs of the nodes in a layer are computed from the outputs of the previous layer, resulting

in the input to the output layer. The output layer is a fully connected layer that composes precisely a node per label class and whose activation function outputs the index of the node with the largest linear activation as the classification decision. In the following we assume the weights of a CNN have been trained.

To fix the notation, we use $[n]$ for $\{1, \dots, n\}$ and $[n_1, n_2]$ for $\{n_1, \dots, n_2\}$. We fix a CNN CNN with a set of layers $[n]$. We assume the nodes in a convolutional layer are arranged into a three dimensional array. Interchangeably we sometimes treat this arrangement as reshaped into a vector. The nodes in a fully connected layer are arranged into a vector. The output of the (j, k, r) -st (j -th, respectively) node in a convolutional (fully connected, respectively) layer i is represented by $x_{j,k,r}^{(i)}$ ($x_j^{(i)}$, respectively). We denote by $\overline{x}^{(i)}$ the vector of all the nodes' outputs in layer i . We write $s^{(i)}$ for the size of layer i and $s_j^{(i)}$ for the size of the j -th dimension of a convolutional layer i .

We now proceed to formally define every layer $2 \leq i \leq n$ as a function $f^{(i)}: \mathbb{R}^{s^{(i-1)}} \rightarrow \mathbb{R}^{s^{(i)}}$ and consequently the CNN composing these. We begin with a fully connected layer i . The layer is associated with a weight matrix $W^{(i)} \in \mathbb{R}^{s^{(i)} \times s^{(i-1)}}$ and a bias vector $\overline{b}^{(i)} \in \mathbb{R}^{s^{(i)}}$. The linear activation of the layer is given by the weighted sum $WS(\overline{x}^{(i-1)}) = W^{(i)} \cdot \overline{x}^{(i-1)} + \overline{b}^{(i)}$. The function computed by the layer can then be defined as $f^{(i)}(\overline{x}^{(i-1)}) = \square(WS(\overline{x}^{(i-1)}))$, where $\square \in \{\text{ReLU}, \text{Argmax}\}$ with the function $\text{ReLU}(x) = \max(0, x)$ being applied element-wise to the linear activation. We now give the definition of a convolutional layer i . The layer is associated with a group $\text{Conv}^{(i),1}, \dots, \text{Conv}^{(i),k}$ of $k \geq 1$ convolutions and a max-pooling function $\text{Pool}^{(i)}$. Each convolution $\text{Conv}^{(i),j}: \mathbb{R}^{s^{(i-1)}} \rightarrow \mathbb{R}^{(s_1^{(i-1)}-p+1) \times (s_2^{(i-1)}-q+1)}$ is parameterised over a weight matrix (kernel) $K^{(i),j} \in \mathbb{R}^{p \times q \times s_3^{(i-1)}}$, where $p \leq s_1^{(i-1)}$, $q \leq s_2^{(i-1)}$, and a bias vector $\overline{b}_j^{(i)}$. The (u, v) -st output of the j -st convolution is given by $\text{Conv}_{u,v}^{(i),j}(\overline{x}^{(i-1)}) = K^{(i),j} \cdot \overline{x}_{[u,u'],[v,v'],[s_3^{(i-1)}]}^{(i-1)} + \overline{b}_j^{(i)}$, where $u' = u + p - 1$ and $v' = v + q - 1$. Given the outputs of each of the convolutions, the linear activation of the layer $\text{Conv}^{(i)}: \mathbb{R}^{s^{(i-1)}} \rightarrow$

$\mathbb{R}^{(s_1^{(i-1)}-p+1) \times (s_2^{(i-1)}-q+1) \times k}$ forms a three-dimensional matrix, i.e. $\text{Conv}^{(i)} = \begin{bmatrix} \text{Conv}_1^{(i)} & \dots & \text{Conv}_k^{(i)} \end{bmatrix}$. The non-linear activation of the layer is then computed by the application of the ReLU function. In the final phase, the max-pooling function collapses neighborhoods of size $p' \times q'$ of the latter activations to their maximum values. Formally, $\text{Pool}^{(i)}: \mathbb{R}^{u \times v \times r} \rightarrow \mathbb{R}^{\frac{u}{p'} \times \frac{v}{q'} \times r}$, where $u = (s_1^{(i-1)} - p + 1)$ and $v = (s_2^{(i-1)} - q + 1)$, is defined as follows: $\text{Pool}_{u,v,r}^{(i)} = \max \left(\text{Conv}_{[(u-1)p+1, u \cdot p], [(v-1)q+1, v \cdot q], r}^{(i)} \right)$. The function computed by the layer is then defined by $f^{(i)}(\bar{x}^{(i-1)}) = \text{Pool}^{(i)} \left(\text{ReLU} \left(\text{Conv}^{(i)} \left(\bar{x}^{(i-1)} \right) \right) \right)$.

Given the above a convolutional neural network can be defined as the composition of fully connected and convolutional layers.

Definition 1 (Convolutional neural network). *A convolutional neural network $CNN: \mathbb{R}^{\alpha \times \beta \times \gamma} \rightarrow [c]$ is defined as*

$$CNN(\bar{im}) = f^{(n)}(f^{(n-1)}(\dots f^{(1)}(\bar{x}) \dots))$$

where $\bar{im} \in \mathbb{R}^{\alpha \times \beta \times \gamma}$, $f^{(1)}, \dots, f^{(n-1)}$ are either ReLU fully connected or convolutional layers, $f^{(n)}$ is an Argmax fully connected layer, and $[c]$ is a set of class labels.

Image transformations. We briefly describe affine and photometric transformations. An affine transformation is a mapping between affine spaces that preserves collinearity and ratios of distances [11]. It is represented in vector algebra as follows.

$$\begin{pmatrix} x' \\ y' \\ 1 \end{pmatrix} = \begin{bmatrix} a_{11} & a_{12} & t_x \\ a_{21} & a_{22} & t_y \\ 0 & 0 & 1 \end{bmatrix} \begin{pmatrix} x \\ y \\ 1 \end{pmatrix}$$

where (x, y) is a point, $A = \begin{bmatrix} a_{11} & a_{12} \\ a_{21} & a_{22} \end{bmatrix}$ is a non-singular matrix, and $\bar{t} = (t_x, t_y)^T$ is the translation vector.

An affine transformation whereby A equals the identity matrix is said to be a *translation*. An affine transformation is referred to as *scaling* if $A = \sigma I$, $t_x = 0$ and $t_y = 0$ for a scale factor σ . In the case where $\sigma < 1$ the scaling is called *subsampling*, whereas in the case where $\sigma > 1$ the scaling is known as *zooming*. Given a transformation \mathfrak{T}

we write $\text{doff}(\mathfrak{T})$ for the tuple of degrees of freedom in \mathfrak{T} , e.g., if \mathfrak{T} is a translation, then $\text{doff}(\mathfrak{T}) = (t_x, t_y)$. Given $d \in \mathbb{R}^{|\text{doff}(\mathfrak{T})|}$, we denote by $\mathfrak{T}[d]$ the *concretisation* of \mathfrak{T} whereby every parameter $\text{doff}(\mathfrak{T})_i$ is set to d_i . In this paper we consider translations and scaling transformations, both in isolation and in composition with themselves.

A photometric transformation is an affine change in the intensity of the pixels [21]. It is defined as $f(p) = \alpha p + \beta$. If $0 < \alpha < 1$, then the transformation reduces the contrast of the image. Otherwise, if $\alpha > 1$, the transformation increases the contrast of the image. The factor β controls the luminosity of the image with higher values pertaining to brighter images.

3 Local transformational robustness

CNNs are known to be susceptible to adversarial attacks. Slight perturbations of an image, even imperceptible to the human eye, can cause the misclassification of the image [17]. As mentioned in the introduction a recent body of work aims at establishing the *adversarial local robustness* of neural networks against said attacks by adopting a verification perspective [16, 7, 12, 13]. Specifically, given an image \bar{im} , current state-of-the-art methods check whether all images \bar{im}' with $\|\bar{im}' - \bar{im}\|_p \leq \delta$, for some L_p -norm, are classified as belonging to the same class with \bar{im} . While this approach can effectively identify probable misclassification when images marginally differ, e.g., by a few different pixels, we argue that it is not adequate to identify a much wider class of variations to an image that should not affect its classification.

Intuitively, a perception system should be assessed as robust whenever it assigns the same label to every pair of images that human perception finds indistinguishable. For instance, autonomous vehicles are expected to correctly identify objects irrespective of the angle and position of the camera, the environment light conditions, the position of the object in the image, the distance of the object from the camera, etc. It follows that the *classification decision should be the same irrespective of minor translations, scaling, and photometric transforms of the image from the camera* (Figure 1).

Crucially, adversarial local robustness depends on the

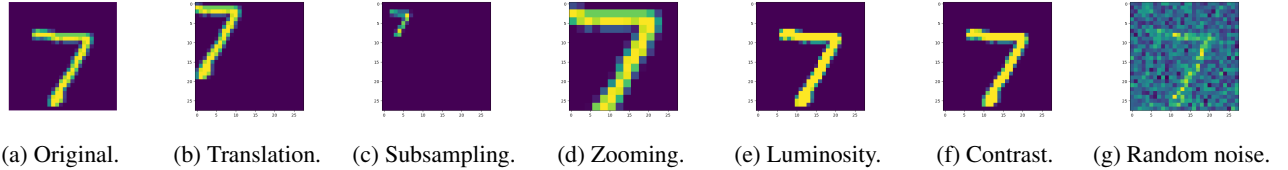


Figure 1: Affine and photometric transformations applied on an image from the MNIST dataset.

encapsulation of all indistinguishable images within the space induced by bounding some distance metric, typically the infinity norm. Consequently, in order to capture said transformations in present approaches, the bound on the distance between the images has to be so large that, intuitively, distinguishable images would have to be classified in the same way to meet the predefined distance.

For example, consider Figure 1. The L_∞ -norm between the original image and the brightened image is 17.16, whereas the distance between the original image and the image composed with random noise is 16.02. Clearly the brightened image should be classified as the original one whereas the classification of the noisy one is not as clear. Following these observations, we propose the formal verification of the robustness of CNNs not just up to a distance metric, but up to transformations. We call this the *transformational robustness property*.

Definition 2 (Local transformational robustness). *A convolutional neural network CNN is said to be locally transformationally robust for an image \bar{i}_m and a transformation \mathfrak{T} with domain $\mathcal{D} \subseteq \mathbb{R}^{|\text{doff}(\mathfrak{T})|}$ if for all $d \in \mathcal{D}$ we have that $CNN(\mathfrak{T}[d](\bar{i}_m)) = CNN(\bar{i}_m)$.*

In other words, we say that CNN is locally transformationally robust if the image in question is classified in the same way following the transformation under analysis. The emphasis on “local” in the definition above follows [13, 16] and refers to the fact that the property is relative to a single image. In contrast, global transformational robustness is defined independently of the image. We do not add this definition as the method provided below only deals with local properties. Also note that the definition above is parameterised over a domain for the values of the parameters. Indeed, for verification purposes, it may be preferable to check only a range of values, e.g., in photometric transformations it is typically not relevant to consider the transformation for which every pixel is mapped

to the black colour. Hereafter, we assume that the transformation domain is a linearly definable set.

4 Verifying local transformational robustness

In this section we develop a procedure for verifying local transformational robustness by recasting the problem into MILP. The procedure takes as input a trained CNN CNN , an image \bar{i}_m with class label $l_{\bar{i}_m}$, and a sequence of k transformations $\mathfrak{T}^{(1)}, \dots, \mathfrak{T}^{(k)}$ with domains $\mathcal{D}^{(1)}, \dots, \mathcal{D}^{(k)}$, respectively. It then constructs an *transformational CNN* \overline{CNN} by treating the transformations as additional layers and appending them to the input layer. More precisely, $\overline{CNN} = f^{(n+k+2)}(\dots f^{(1)}(\dots))$, where $f^{(n+k+2)}, \dots, f^{(k+2)}$ are the original layers of CNN , $f^{(k+1)}$ is a *perturbation layer* and $f^{(k)}, \dots, f^{(1)} = \mathfrak{T}^{(k)}, \dots, \mathfrak{T}^{(1)}$. The perturbation layer helps to simulate subpixel transformations; this will be discussed below. The transformational CNN is then encoded into mixed-integer linear constraints layer by layer. For each layer and transformation i we now give the set of linear constraints $\mathcal{C}^{(i)}$ characterising the various layers and transformations that we consider.

Photometric transformations. We begin by presenting the mixed-integer linear encodings for photometric transformations. A photometric transformation has two degrees of freedom: the factor μ that handles the contrast of the image, and the factor ν which controls the luminosity of the image. We assume the minimum value of a pixel is 0 and write p_{max} for its maximum value. The possible instantiations of a photometric transformation are ex-

pressed by the following linear constraints.

$$\lambda_d \geq \min_d(\mathcal{D}^{(i)}) \text{ and } \lambda_d \leq \max_d(\mathcal{D}^{(i)}), d \in \text{dof}(\mathfrak{T}^{(i)}) \quad (C_1)$$

where each λ_d is an LP variable controlling the values of the factor d , and $\min_d(\mathcal{D}^{(i)})$ ($\max_d(\mathcal{D}^{(i)})$, respectively) denotes the minimum (maximum, respectively) value for the factor d in $\mathcal{D}^{(i)}$. To encode the result of a photometric transformation on a pixel we simply express the corresponding linear operation.

$$\mathfrak{T}_{px}^{(i)}(\bar{x}^{(i-1)}) = \mu \cdot \bar{x}_{px}^{(i-1)} + \nu \quad (C_2)$$

Given this, the linear encoding of a photometric transformation $\mathfrak{T}^{(i)}$ is then given by the set of constraints $\mathcal{C}^{(i)} = C_1 \cup C_2$.

Affine transformations. We now turn to translating affine transformations. For each case we use a set of constraints of the form C_1 capturing the set of possible instantiations of the transformation. Also, for each case, we introduce a binary variable $\delta_d^{(i)}$ for every instantiation d . The variable represents whether the corresponding instantiation is the one being applied. At any time we assume the application of precisely one instantiation by imposing the constraint:

$$\sum_{d \in \mathcal{D}^{(i)}} \delta_d^{(i)} = 1 \quad (C_3)$$

We also force a bijection between the set of δ variables and the instantiations they represent by assuming:

$$\sum_{d \in \mathcal{D}^{(i)}} d_j \cdot \delta_d^{(i)} = \lambda_j \text{ for each d.o.f. } j \text{ in } \mathfrak{T}^{(i)} \quad (C_4)$$

So $\delta_d^{(i)} = 1$ iff, for each d.o.f. j , the LP variable λ_j representing j equals d_j .

We now present the encodings of each of the transformations. We begin by considering geometric translation. A translation shifts the location of every pixel as per the translation vector (u', v') :

$$\mathfrak{T}_{u',v'}^{(i)}(\bar{x}^{(i-1)}) = \sum_{(u'',v'') \in \mathcal{D}^{(i)}} \bar{x}_{u+u'',v+v'',r}^{(i-1)} \cdot \delta_{u'',v''}^{(i)} \quad (C_5)$$

Therefore, the linear encoding for a translation $\mathfrak{T}^{(i)}$ is defined as $\mathcal{C}^{(i)} = C_1 \cup C_3 \cup C_4 \cup C_5$.

Next we consider subsampling. The transformation collapses neighbourhoods of points to a point whose value is a statistic approximation of the neighbourhood. Here we consider the arithmetic mean value. The size of the neighbourhood is controlled by the scaling factor d .

$$\mathfrak{T}_{u,v,r}^{(i)}(\bar{x}^{(i-1)}) = \sum_{d \in \mathcal{D}^{(i)}} \text{AM}(\bar{x}_{[(u-1)d, u \cdot d], [(v-1)d, v \cdot d], r}^{(i-1)}) \cdot \delta_d^{(i)} \quad (C_6)$$

It follows that the linear encoding for a subsampling $\mathfrak{T}^{(i)}$ is defined as $\mathcal{C}^{(i)} = C_1 \cup C_3 \cup C_4 \cup C_6$.

Lastly, we consider zooming. Zooming replicates the value of a pixel to a rectangular neighbourhood of pixels. The value of the neighbourhood is controlled by the scaling factor d .

$$\mathfrak{T}_{u,v,r}^{(i)}(\bar{x}^{(i-1)}) = \sum_{d \in \mathcal{D}^{(i)}} \bar{x}_{\lceil \frac{u}{d} \rceil, \lceil \frac{v}{d} \rceil, r}^{(i-1)} \cdot \delta_d^{(i)} \quad (C_7)$$

Therefore, the linear encoding for a zooming $\mathfrak{T}^{(i)}$ is defined as $\mathcal{C}^{(i)} = C_1 \cup C_3 \cup C_4 \cup C_7$.

Perturbations. Next we describe the linear encoding of the perturbation layer. The layer is introduced to simulate subpixel transformations. Whereas interpolation can be recast to MILP so as compute the transformations, the number of binary variables needed for the encoding is overwhelming w.r.t the performance of the verifier, as also showed by implementations we developed. In contrast, the perturbation layer results in a conciser program whereby only two inequalities per pixel are used. The layer perturbs each pixel within an L_∞ norm-ball. Given the radius of the norm-ball is sufficiently big, i.e., equal to the variance of the image, the layer captures each of the images that could be computed via interpolations. Consequently it enables the derivation of stronger robustness guarantees than the ones that could be given by using a specific interpolation. The linear encoding of the layer is given for each pixel px by the following constraints.

$$\bar{x}_{px}^{(k+1)} - \bar{x}_{px}^{(k)} \leq \rho \quad (C_8)$$

$$\bar{x}_{px}^{(k+1)} - \bar{x}_{px}^{(k)} \geq -\rho \quad (C_9)$$

where ρ is a given radius.

We now consider the encodings of the layers of the CNN under question. We separately translate these phase by phase.

Fully connected layer. We give the MILP description of the weighted sum and ReLU functions. We do not directly represent the Argmax function since the function is not essential in expressing the local transformational robustness properties that we are here concerned with (see below). The weighted sum function is given by the following:

$$\text{WS}_j(\bar{x}^{(i-1)}) = W_j^{(i)} \cdot \bar{x}_j^{(i-1)} + \bar{b}_j^{(i)} \quad (C_{10})$$

To capture the piecewise-linearity of the ReLU function we introduce a binary variable $\delta_j^{(i)}$ per node j that represents whether the output of the node is above 0 [1].

$$\text{ReLU}_j(\bar{x}^{(i-1)}) \geq 0 \quad (C_{11})$$

$$\text{ReLU}_j(\bar{x}^{(i-1)}) \geq \text{WS}_j(\bar{x}^{(i-1)}) \quad (C_{12})$$

$$\text{ReLU}_j(\bar{x}^{(i-1)}) \leq \text{WS}_j(\bar{x}^{(i-1)}) + M\delta_j^{(i)} \quad (C_{13})$$

$$\text{ReLU}_j(\bar{x}^{(i-1)}) \leq M(1 - \delta_j^{(i)}) \quad (C_{14})$$

Above M is a sufficiently large number. Therefore the linear encoding of a fully connected layer i is defined by $\mathcal{C}^{(i)} = C_{10} \cup \dots \cup C_{14}$.

Convolutional layer. In addition to the ReLU phase, a convolutional layer includes a convolution and a max-pooling phase. Similarly to the weighted-sum function, a convolution is a linear operation on the input of the layer and can be encoded by the following:

$$\begin{aligned} \text{Conv}_{u,v}^{(i),j}(\bar{x}^{(i-1)}) &= K_j^{(i)} \cdot \bar{x}_{[u,u'],[v,v'],[s_3^{(i-1)}]}^{(i-1)} + \bar{b}_j^{(i)}, \\ u' &= u + p - 1, v' = v + q - 1. \end{aligned} \quad (C_{15})$$

A max-pooling function is parameterised over the size of the groups of pixels over which the max-pooling is performed. Previous linear encodings of the function use a binary variable per node in a group [5]. We here provide an encoding that uses logarithmically less variables. Specifically, to select the maximum value from a group we introduce a sequence of binary variables. The sequence's binary number expresses the node in a group whose value is maximum. Since the size of the group

is $p \cdot q$ we use $\lceil \log_2(p \cdot q) \rceil$ variables. To facilitate the presentation of the corresponding linear constraints, we write \mathbf{n} for the binary representation of $n \in \mathbb{Z}$. We denote by $|\mathbf{n}|$ the number of binary digits in \mathbf{n} . Given $j \in |\mathbf{n}|$, \mathbf{n}_j expresses the j -th digit in \mathbf{n} whereby the first digit is the least significant bit. If $j > |\mathbf{n}|$, then we assume that $\mathbf{n}_j = 0$. The linear representation of the max-pooling function for a pixel $px = (px_\alpha, px_\beta, px_\gamma)$ and pool size $p \times q$ is given by the following.

$$\begin{aligned} \text{Pool}_{px}^{(i)} &\geq \text{Conv}_{(px_\alpha-1)p+u',(px_\beta-1)q+v',px_\gamma}^{(i)} \\ u' &\in [p], v' \in [q] \end{aligned} \quad (C_{16})$$

$$\begin{aligned} \text{Pool}_{px}^{(i)} &\leq \text{Conv}_{(px_\alpha-1)p+u',(px_\beta-1)q+v',px_\gamma}^{(i)} + \\ &M \sum_{j \in [|\mathbf{p} \cdot \mathbf{q}|]} \mathbf{z}_j + (1 - 2\mathbf{z}_j)\delta_{px,j}^{(i)}, \\ u' &\in [p], v' \in [q], z = (u' - 1)q + v' - 1 \end{aligned} \quad (C_{17})$$

where $\delta_{px,1}^{(i)}, \dots, \delta_{\lceil \log_2(p \cdot q) \rceil}^{(i)}$ are the binary variables associated with px . For the case where $p \cdot q$ is not a power of 2 we require from the number represented by $\delta_{px,1}^{(i)}, \dots, \delta_{\lceil \log_2(p \cdot q) \rceil}^{(i)}$ to lie within $0, \dots, p \cdot q - 1$. The constraint is formally expressed as follows.

$$\begin{aligned} \sum_{j \in [|\mathbf{p} \cdot \mathbf{q}|]} \mathbf{z}_j + (1 - 2\mathbf{z}_j)\delta_{px,q}^{(i)} &\geq 1, \\ z &\in [p \cdot q, 2^{|\mathbf{p} \cdot \mathbf{q}|} - 1] \end{aligned} \quad (C_{18})$$

Example 1. Assume the application of the max-pooling function on a group of nodes x_1, \dots, x_4 . Let y denote the output of the function. Its MILP encoding as per (16)-(19) uses two binary variables δ_1, δ_2 and is given by the following.

$$\begin{aligned} y &\geq x_j, j \in [4] \\ y &\leq x_1 + M(\delta_1 + \delta_2) \\ y &\leq x_2 + M(1 - \delta_1 + \delta_2) \\ y &\leq x_3 + M(\delta_1 + 1 - \delta_2) \\ y &\leq x_4 + M(1 - \delta_1 + 1 - \delta_2) \end{aligned}$$

The linear encoding of a convolutional layer i is defined by $\mathcal{C}^{(i)} = C_{15} \cup \dots \cup C_{18}$.

Given the above, the linear encoding of a transformational CNN can be defined as the union of the linear constraints characterising its layers.

Definition 3 (Linear encoding of transformational CNNs). *The linear encoding of a transformational CNN $\overline{CNN} = f^n(f^{n-1}(\dots f^1(\dots)))$ is defined by $\mathcal{C}^{(\overline{CNN})} = \mathcal{C}^{(1)} \cup \dots \cup \mathcal{C}^{(n)}$.*

We can exploit the above encoding to construct a linear program whose solution corresponds to a solution of the robustness problem for the CNN under analysis. Indeed, we can extend the above encoding to represent the local robustness property.

Local transformational robustness. We now define linear constraints to determine whether there are instantiations for the transformations of the original image \overline{im} whose output is classified differently than \overline{im} . More specifically, we check whether there is a linear activation in the output layer that is larger than the activation associated with the class $l_{\overline{im}}$ of \overline{im} . Similarly to the max-pooling function we express this by introducing a sequence of size $\lceil \log_2 c \rceil$ of binary variables; the sequence's binary number b denotes the node from the output layer that is associated with class $b + 1 \in [c]$ and whose linear activation is larger than the linear activation of the node associated with $l_{\overline{im}}$.

$$\begin{aligned} \text{WS}_{l_{\overline{im}}}(\overline{x}^{(n-1)}) &\leq \text{WS}_j(\overline{x}^{(n-1)}) + \\ M \sum_{k \in [c]} &\left(\mathbf{j}_k + (1 - 2\mathbf{j}_k)\delta_k^{(n)} \right), \\ j &\in [0, c - 1] \setminus \{l_{\overline{im}} - 1\} \end{aligned} \quad (C_{19})$$

Again, we prevent $\delta_0^{(n)}, \dots, \delta_{\lceil \log_2 c \rceil}^{(n)}$ from representing $l_{\overline{im}} - 1$ or any number greater than $c - 1$:

$$\begin{aligned} \sum_{k \in [c]} \mathbf{j}_k + (1 - 2\mathbf{j}_k)\delta_k^{(n)} &\geq 1, \\ j &\in \{l_{\overline{im}} - 1\} \cup [c, 2^{\lceil \log_2 c \rceil} - 1]. \end{aligned} \quad (C_{20})$$

The linear encoding of local robustness is then defined by $\mathcal{C}^{(lrob)} = C_{19} \cup C_{20}$.

In summary, we have shown that all the affine and photometric transformations considered are naturally captured by appropriate sets of linear constraints. Moreover, we have shown that the property of local transformational robustness can naturally be encoded into a set of linear constraints. We now give the main result of this section by formally linking local transformational robustness of a

given CNN with respect to a particular image and a transformation and the lack of a solution for the corresponding MILP problem.

Theorem 1. *Let CNN be a CNN, \mathfrak{T} a transformation with domain \mathcal{D} , and \overline{im} an image. Let LP be the linear problem defined on objective function $obj = 0$ and set of constraints $\mathcal{C}^{(\overline{im})} \cup \mathcal{C}^{(CNN)} \cup \mathcal{C}^{(lrob)}$, where $\mathcal{C}^{(\overline{im})} \triangleq \overline{x}^{(0)} = \overline{im}$ fixes the input of \mathfrak{T} to \overline{im} . Then CNN is locally transformationally robust for \mathfrak{T} and \overline{im} iff LP has no solution.*

Proof. Let $\overline{CNN} = f^{(n+1)}(\dots f^{(1)}(\overline{im}) \dots)$.

For the left to right direction assume that LP has a feasible solution. Consider $d = (\lambda_j : j \in \text{dof}(\mathfrak{T}))$, where each λ_j is the value of the d.o.f. d_j of \mathfrak{T} in the solution. By the definition of LP we have that $CNN(\mathfrak{T}[d](\overline{im})) = \text{Argmax}(\overline{x}^{(n+1)})$. By the definition of $\mathcal{C}^{(lrob)}$ there is l with $l \neq l_{\overline{im}}$ and $\overline{x}_l^{(n+1)} \geq \overline{x}_{l_{\overline{im}}}^{(n+1)}$. Therefore $CNN(\mathfrak{T}[d](\overline{im})) \neq l_{\overline{im}}$, and therefore CNN is not locally transformationally robust.

For the right to left direction suppose that CNN is not locally transformationally robust. It follows that there is $d \in \mathcal{D}$ such that $CNN(\mathfrak{T}[d](\overline{im})) \neq l_{\overline{im}}$. Then, the assignment $\lambda_j = d_j$, for each d.o.f. j of \mathfrak{T} and $\overline{x}_j^{(i)} = (f^{(i)}(\dots f^{(1)}(\overline{im}) \dots))_j$ is a feasible solution for LP . \square

Following the above the local transformational robustness of CNNs can be established whenever the corresponding MILP problem has no solution. Otherwise, if a feasible solution for the problem can be found, then the solution corresponds to the instantiations of the transformations under analysis that violate the robustness of the CNN. From these, it is possible to determine the sets of images responsible for the violation. These exemplars are often called adversarial examples in related literature. Finally note that the result holds for the composition of any finite number of transformations considered in the paper.

We conclude by noting that finding adversarial examples can be used to improve the accuracy of the classifier, e.g., via retraining. On the other hand showing local transformational robustness can be used to build a formal safety case for the perception system in question.

Translation			Subsampling			Zooming			Photometric		
\mathcal{D}	# \checkmark (s)	LTR	\mathcal{D}	# \checkmark (s)	LTR	\mathcal{D}	# \checkmark (s)	LTR	\mathcal{D}	# \checkmark (s)	LTR
$[-1, 1]^2$	5(48)	0	[2, 3]	97(2)	0	[2, 3]	94(3)	4	$[0.01, 0.03] \times [0.99, 1.01]$	100(1.1)	2
$[-3, 3]^2$	63(15)	0	[2, 5]	96(3)	0	[2, 5]	90(1)	7	$[0.01, 0.05] \times [0.97, 1.03]$	100(8.23)	2
$[-5, 5]^2$	87(26)	0	[2, 7]	95(2)	0	[2, 7]	97(4)	2	$[0.01, 0.07] \times [0.9, 1.1]$	100(8.36)	2
$[-7, 7]^2$	90(22)	0	[2, 9]	96(3)	7	[2, 9]	96(3)	7	$[0.1, 0.5] \times [0.7, 1.3]$	100(10.05)	2
$[-9, 9]^2$	90(20)	0	[2, 11]	93(1)	0	[2, 11]	96(3)	7	$[0.1, 0.7] \times [0.5, 1.5]$	97(5.51)	0

Table 1: Experimental results.

5 Implementation and experimental results

We have implemented the procedures from the previous section as a toolkit VENUS [2]. The toolkit takes as input the descriptions of a CNN and a sequence of transformations against which the local transformational robustness of the CNN is meant to be assessed. Following this VENUS builds the linear encoding of the verification query layer by layer and following all the transformations in the input by adding the constraints discussed in the preceding Section.

Having constructed the linear program the verifier invokes the Gurobi checker [10] to ascertain whether the program admits a solution. The *satisfiability* output of the latter corresponds to the violation of the local transformational robustness property of the CNN, whereas the *unsatisfiability* output can be used to assert the CNN is transformationally locally robust.

We have tested VENUS on networks trained on the MNIST dataset [14] using the deep learning toolkit Keras [4]. To the best of our knowledge currently there are no other methods or tools for the same problem; so, in what below we report only the results obtained with VENUS. In the experiments we fixed a CNN of 1481 nodes, with a convolutional layer of 3 convolutions with kernels of size 15×15 and pool-size 2×2 , and an output layer with 10 nodes. The accuracy of the network on the MNIST dataset is 93%. To check the network’s transformational local robustness we selected 100 images for which the network outputs the correct classification label. We then performed experiments for all of the transformations with varying domains for each of their degrees of freedom. The experiments were run on a machine equipped with an i7-7700 processor and 16GB of RAM and running Linux kernel version 4.15.0. Table 1 sum-

marises the results.

For every transformation and its domains considered, we report the number of images that have been verified (irrespective of whether these were shown robust) under the timeout of 200s followed by the average time taken for verifying said images. This is indicated in the column # \checkmark (s). For example, for subsampling transformations on domain [2, 3], the method could verify 97 images out of 100 with an average time of 2 secs. Following this, in the LTR column we report the number of these that were assessed locally transformationally robust.

Note that there is some variability in the results. For example, several images could not be assessed by the timeout for the translation with domain $[-1, 1]$ but many more could be analysed under the translation domain $[-3, 3]$. This is likely to be due to optimisations carried out by Gurobi which can be applied in some cases only. Indeed, note in general that an increase in the range of the domains does not lead to longer computations times, since the resulting linear program is only marginally extended.

In summary, the results show that the CNN built from the MNIST dataset is not locally transformationally robust with respect to translation, subsampling and zooming, returning different classifications even for small transformational changes to the input. The CNN appears just as fragile in terms of luminosity and contrast changes. Overall, the results show that the CNN in question is brittle with respect to transformational robustness. We stress that the aim of this work is not to build robust CNNs, but to provide a provably correct and automatic method that can be used to make this assessment systematically. If the CNN that we analysed was intended to be used in as part of a perception module in a safety-critical autonomous system, our analysis would suggest that the CNN may be inadequate.

Still, in the spirit of adversarial retraining, the tech-

nique here described can be used to augment the training set so as to improve the robustness of the network under analysis [9]. To test this we trained a CNN with images from the MNIST dataset (60000 images) and recorded its classification accuracy as 19% on transformed MNIST images. We then used VENUS to generate over 10000 transformed images (for compositions of transformations here considered) which we appended to the training set. The augmented set was then used to retrain the network resulting in a classification accuracy of 26%. This exemplifies VENUS not only as a verification tool but also as a tool to improve the robustness of CNNs.

We conclude by noting that we conducted further tests with images of different sizes. As expected, we found that the effectiveness of the toolkit is hindered by increases in the size of the network, as these lead to heavier MILP encodings. This has already been reported in the literature [5] and points to further work to improve scalability further.

6 Conclusions

Forthcoming autonomous systems are expected to rel. aspects of modern society. Several of these, including autonomous vehicles, are effectively safety-critical systems, i.e., they are systems in which malfunctions may lead to loss of life. Differently for other non-autonomous safety-critical systems, such as avionics systems, no methods presently exist to give formal guarantees to large classes of autonomous systems. Providing formal guarantees for autonomous systems in which learning-enabled components are present (i.e., components synthesised from data via machine learning methods) is presently an open challenge. We believe that research is urgently needed to address this deficiency.

To this end, in this paper we have considered a class of perception systems often present in autonomous systems, i.e., CNN-based classifiers commonly used in the perception modules of autonomous systems. While CNNs are regularly used in various applications where their correctness and accuracy is not essential, their use in autonomous systems requires a high degree of assurance. Typically this is either directly provided by, or aided by formal methods, as in the case of DO-333/ED-216 in avionics. This is also likely to be required for certification purposes

of the system.

To this end, we have introduced a notion of robustness, called local transformational robustness, which can be used to give guarantees on the perception system under analysis. Local transformational robustness encodes the ability of a classifier to withstand variations of the image in question with respect to its classification. These modifications, encoded mathematically as various kinds of transformations, are meant to capture those induced by the normal variability of devices and environment conditions at runtime. We developed a method to assess local transformational robustness automatically by translating this to MILP problems. The experimental results showed that the toolkit we introduced returns correct and viable results against the MNIST dataset for all the transformations considered.

In further work, firstly, we plan to improve the performance of the back-end for the problems considered including experimenting with other technologies such as SMT and mixed approaches. Secondly, while we focused on local properties in this paper, i.e., properties concerning a single image, we intend to extend the work to study (global) robustness with respect to classes of images. Lastly, while the paper focused on images, the notion of local transformational robustness is general to be applied in other contexts where CNNs are used including audio recognition.

Acknowledgements. The authors would like to thank Daniel Rueckert and Rahul Sukthankar for comments on a previous version of this article. This work is partly funded by DARPA under the Assured Autonomy programme.

References

- [1] M. Akintunde, A. Lomuscio, L. Maganti, and E. Pirovano. Reachability analysis for neural agent-environment systems. In *Proceedings of the 16th International Conference on Principles of Knowledge Representation and Reasoning (KR18)*, pages 184–193. AAAI Press, 2018.
- [2] Anonymous. *Venus*; supplementary material, 2018.
- [3] C. Bishop. *Pattern Recognition and Machine Learning*. Springer, 2006.
- [4] F. Chollet. Keras. <https://keras.io>, 2015.
- [5] K. Dvijotham, R. Stanforth, S. Goyal, T. Mann, and P. Kohli. A dual approach to scalable verification of deep networks. *arXiv preprint arXiv:1803.06567*, 2018.

- [6] R. Ehlers. Formal verification of piece-wise linear feed-forward neural networks. In *Proceedings of the 15th International Symposium on Automated Technology for Verification and Analysis (ATVA17)*, volume 10482 of *Lecture Notes in Computer Science*, pages 269–286. Springer, 2017.
- [7] T. Gehr, M. Mirman, D. Drachler-Cohen, P. Tsankov, S. Chaudhuri, and M. Vechev. AI²: Safety and robustness certification of neural networks with abstract interpretation. In *2018 IEEE Symposium on Security and Privacy (S&P18)*, pages 948–963, 2018.
- [8] A. Goodfellow, Y. Bengio, and A. Courville. *Deep learning*, volume 1. MIT press Cambridge, 2016.
- [9] I. Goodfellow, J. Shlens, and C. Szegedy. Explaining and harnessing adversarial examples (2014). *arXiv preprint arXiv:1412.6572*.
- [10] Z. Gu, E. Rothberg, and R. Bixby. Gurobi optimizer reference manual. <http://www.gurobi.com>, 2016.
- [11] R. Hartley and A. Zisserman. *Multiple view geometry in computer vision*. Cambridge university press, 2003.
- [12] X. Huang, M. Kwiatkowska, S. Wang, and M. Wu. Safety verification of deep neural networks. In *Proceedings of the 29th International Conference on Computer Aided Verification (CAV17)*, volume 10426 of *Lecture Notes in Computer Science*, pages 3–29. Springer, 2017.
- [13] G. Katz, C. W. Barrett, D. L. Dill, K. Julian, and M. J. Kochenderfer. Reluplex: An efficient SMT solver for verifying deep neural networks. In *Proceedings of the 29th International Conference on Computer Aided Verification (CAV17)*, volume 10426 of *Lecture Notes in Computer Science*, pages 97–117. Springer, 2017.
- [14] Y. LeCun, L. Bottou, Y. Y. Bengio, and P. Haffner. Gradient-based learning applied to document recognition. *Proceedings of the IEEE*, 86(11):2278–2324, 1998.
- [15] A. Lomuscio and L. Maganti. An approach to reachability analysis for feed-forward relu neural networks. *CoRR*, abs/1706.07351, 2017.
- [16] N. Narodytska, S. P. Kasiviswanathan, L. Ryzhyk, M. M. Sagiv, and T. Walsh. Verifying properties of binarized deep neural networks. *arXiv preprint arXiv:1709.06662*, 2017.
- [17] N. Papernot, P. McDaniel, S. Jha, M. Fredrikson, Z. B. Celik, and A. Swami. The limitations of deep learning in adversarial settings. In *Security and Privacy (EuroS&P), 2016 IEEE European Symposium on*, pages 372–387. IEEE, 2016.
- [18] K. Pei, Y. Cao, J. Yang, and S. Jana. Towards practical verification of machine learning: The case of computer vision systems. *CoRR*, abs/1712.01785v3, 2017.
- [19] O. Russakovsky, J. Deng, H. S. J. Krause, S. Satheesh, M. S. Z. Huang, A. Karpathy, A. Khosla, and M. Bernstein. Imagenet large scale visual recognition challenge. *International Journal of Computer Vision*, 115(3):211–252, 2015.
- [20] S. Seshia, A. Desai, T. Dreossi, D. Freemont, S. Ghos, E. Kim, S. Shivakumar, M. Vazquez-Chanlatte, and X. Yue. Formal specification for deep neural networks. Technical report, EECS. University of California at Berkeley, 2018.
- [21] M. Sonka, V. Hlavac, and R. Boyle. *Image processing, analysis, and machine vision*. Cengage Learning, 2014.